Hindawi
Journal of Chemistry
Volume 2020, Article ID 1241952, 11 pages
https://doi.org/10.1155/2020/1241952

Research Article

Selective Allylic Oxidation of Terpenic Olefins Using Co-Ag Supported on SiO_2 as a Novel, Efficient, and Recyclable Catalyst

Abderrazak Aberkouks,[1,2] Ayoub Abdelkader Mekkaoui,[1,2] Mustapha Ait Ali,[2] Larbi El Firdoussi,[2] and Soufiane El Houssame[1]

[1]*Laboratoire de Chimie, Modélisation et Sciences de L'Environnement, Université Sultan Moulay Slimane, Faculté Polydisciplinaire de Khouribga, B. P. 145, 25000 Khouribga, Morocco*
[2]*Laboratoire de Chimie de Coordination et de Catalyse, Département de Chimie, Faculté des Sciences Semlalia, B. P. 2390, 40001 Marrakech, Morocco*

Correspondence should be addressed to Soufiane El Houssame; hous_soufiane@hotmail.com

Received 2 October 2019; Revised 19 December 2019; Accepted 24 December 2019; Published 24 January 2020

Academic Editor: Andrea Penoni

Co-Ag supported on the SiO_2 catalyst was synthesized by the sol-gel method and characterized using XRD, FT-IR, TG-DTG, BET, CV, and SEM/EDX analysis. The catalytic performance of the resulting catalyst was examined by the oxidation of mono and sesquiterpenic olefins using hydrogen peroxide and *tert*-butyl peroxide as oxidant agents. Various parameters such as catalyst amount, temperature, and solvents have been studied. The Co-Ag supported on the SiO_2 catalyst showed a high activity, selectivity, and recyclability for the selected oxidation reaction.

1. Introduction

Solid catalysts are used for converting a vast array of chemicals and fuels, and contribute significantly to economic progress [1, 2]. Recently, the development of solid materials in catalytic oxidation has attracted an economic and ecologic interest because of their easy recovery and the possibility of regeneration which results in a reduction of the environmental impact [3–5]. Moreover, glasses doped with transition metals formed one important class of materials in catalysis field [6]. Among the methods of preparation, sol-gel affords solid materials with high surface area and homogeneity [7]. A high-level incorporation of active metals in the ceramic matrix can be obtained using the sol-gel method than conventional impregnation methods [8].

The allylic oxidation of mono and sesquiterpenic natural olefins, cheap constituents of essential oil extracted from plants [9], constitutes a great route for the synthesis of a wide range of oxygenated products with high added values such as aldehydes, alcohols, ketones, esters, ethers, and phenols [10]. The oxygenated compounds are used in perfumery, aromatherapy, flavoring industry, fine chemical synthesis, food industry, and therapeutic drug [11, 12]. In addition, verbenone is a precursor for the synthesis of taxol used in the treatment of ovarian cancer [13]. The nootkatone, a much popular product replacing the orange aroma [14], was synthesized from β-pinene [15].

The allylic oxidation of terpenic olefins catalyzed by palladium complexes was the subject to various studies [16, 17], and the development of eco-friendly process using eco-compatible reagents and/or metal catalysts in green solvents remained a strong challenge [18]. However, various catalytic systems using molecular complexes [19, 20] or heterogeneous catalysts [21–23] were limited by the use of toxic organic solvents, high amount of oxidants, long reaction time, and difficult catalyst's recovery.

However, in recent years, bimetallic nanoparticles as catalysts instead of monometallic ones are of a great interest from both scientific and technological point of view. In bimetallic catalysts, the electronic effect plays an important role which describes the charge transfer and alloying of the constituting elements can result in the structural changes of

the bimetallic nanoparticles. Therefore, bimetallic nanoparticles may be more effective, more stable, and more selective heterogeneous catalysts due to the synergistic effects occurring between the two different metals [24–27].

Moreover, recently, we have developed Co-Ag codoped ZnO as heterogeneous coordination catalysts for selective oxidation of styrene. Among $Zn_{1-x-y}Ag_xCo_yO$ prepared nanocatalysts, the monometallic ones (Ag-doped ZnO and Co-doped ZnO) are much less efficient [28].

As part of our ongoing research on the development of new heterogeneous nanocatalytic systems [29] as well as the allylic functionalization of natural terpenes [28, 30], herein we report the preparation of 1 mol% Co-1 mol% Ag supported on SiO_2 by the sol-gel method as a novel catalyst in the oxidation reaction. The physiochemical properties of the prepared catalyst were examined by XRD, FT-IR, TG-DTG, BET, and SEM/EDX analysis. It showed a good activity and recyclability for the oxidation of terpenic olefins to their oxygenated derivatives using hydrogen peroxide and *tert*-butyl peroxide as oxidant agents.

2. Experimental Details

2.1. Materials. Tetraethyl orthosilicate (TEOS 99.99%), cobalt nitrate hexahydrate ($Co(NO_3)_2{\cdot}6H_2O$), silver nitrate ($Ag(NO_3)$), nitric acid (HNO_3 67%), (+)–α-pinene (≥99%), (+)-β-pinene (98%), (R)-(+)-limonene (97%), (+)-valencene (≥70%), hydrogen peroxide (30 wt%), *tert*-butyl hydroperoxide (70%), acetonitrile, hexane, ethyl acetate, acetone, chloroform, ethanol, and methanol were purchased from Sigma-Aldrich (of chemical reagent grade) and used as received.

2.2. Characterization. Thermogravimetric analysis (TGA) was recorded on a TA Instrument Q500 apparatus in the flowing air at a heating rate of 10°C min^{-1}. BET-specific surface areas and average pore diameter of the prepared catalyst were measured by N_2 adsorption-desorption technique using the Micromeritics analyser P/N 05098-2.0 Rev A. The stretching vibration frequencies of the catalyst were recorded by FT-IR spectroscopy in the range of 400–4000 cm^{-1} using a Bruker vertex70 DTGS. Spectrometer XRD measurements were performed on a XPERT-MPD Philips diffractometer using Cu-K α radiation as the X-ray source in the 2θ range of 20°–80°. The size, morphology, and elemental mapping of the microstructures were carried out on VEGA3 TESCAN microscope equipped with an energy dispersive X-ray spectrometer (EDAX TEAM). The cyclic voltammetry (CV) study was performed between 1500 mV/−500 mV and 300 mV/−200 mV with a carbon paste electrode modified by our prepared catalyst in a 0.1 M HCl electrolyte at a scan rate of 100 mV·s^{-1} at room temperature.

2.3. Catalyst Preparation. A detailed preparation of SiO_2 by the sol-gel method is described in the literature [31–33]. The preparation was carried out as follows: a mixture of 10.4 g of tetraethyl orthosilicate (TEOS), 4.6 g of ethanol, and 4.6 g of 0.15 M nitric acid was stirred for 1 hour at room temperature. The resulting clear solution was combined with needed amount of $Co(NO_3)_2{\cdot}6H_2O$ and $Ag(NO_3)$ dissolved in 4.6 g of ethanol, stirred for 1 h at room temperature, and dried at 80°C for 24 hours. The dried gel was ground into fine powders and calcined at 600°C for 5 h under the air to obtain nanopowders of 1 mol% Co-1 mol% Ag supported on SiO_2.

2.4. Catalytic Activity. A 50 mL rotaflow tube equipped with magnetic stirring and immersed in bath oil at 80°C was used to mix 0.5 mL of the substrate (terpenic olefin), 0.1 g of nanocatalyst (Co-Ag supported SiO_2), and 5 mL of acetonitrile. Then, 1.3 mL of H_2O_2 (30% wt) was added, and the resulting solution was stirred at 80°C. The reaction process was monitored using gas chromatography (GC) equipped with a FID using an Rtx-5 capillary column. Dodecane was used as an internal standard for the quantitative analysis of the reaction products. After completion of the reaction, 5 mL of distilled water was added to the residue and extracted with ethyl acetate (3 × 10 ml). The combined organic phases were dried over $MgSO_4$ and evaporated under reduced pressure. The catalyst was separated from the reaction mixture, washed, dried, and then reused for further use.

3. Results and Discussion

3.1. Catalyst Characterization. The XRD pattern generated by 1 mol% Co-1 mol% Ag supported SiO_2 is shown in Figure 1. The wide peaks between 18° and 40° associated with the crystalline phase are not revealed as it was intended for an amorphous structure [34–36]. Based on the XRD study, the amount of the doped metal does not affect the amorphous structure of silica.

Thermogravimetric analysis of the Co-Ag/SiO_2 nanocatalyst studied the loss of mass as a function of temperature. The TG-DTG curves of the precursor obtained by the sol-gel method revealed a thermal event (Figure 2). The peak located at 150°C corresponds to a loss of crystal water from the catalyst (3.5%).

The BET (Brunauer-Emmett-Teller) analysis of 1 mol% Co-1 mol% Ag supported on the SiO_2 catalyst was performed. The specific surface area of the catalyst was determined to be 306.18 m^2/g, and the calculated BJH pore size was 7.87 nm. The nitrogen adsorption/desorption isotherm diagram and the pore size distribution diagram are shown in Figures 3 and 4. The sample corresponds to a type IV isotherm and hysteresis type H1 in the Brunauer classification. This type of diagram has been attributed to the predominance of mesopores, and the pore sizes are in the range between 2 and 14 nm.

Structural characterization of the nanocatalyst 1 mol% Co-1 mol% Ag supported on SiO_2 was also performed using FT-IR data, based on the spectrum shown in Figure 5. The band at 460 cm^{-1} corresponds to the bending mode of the Si-O-Si bonds. The peaks at 806 cm^{-1} and 1080 cm^{-1} bands are, respectively, attributed to the symmetric and asymmetric stretching modes of these links [37, 38]. The bands at 960 cm^{-1} and 1650 cm^{-1} are assigned to the Si-OH groups and the physisorbed water in the sample [39], while the

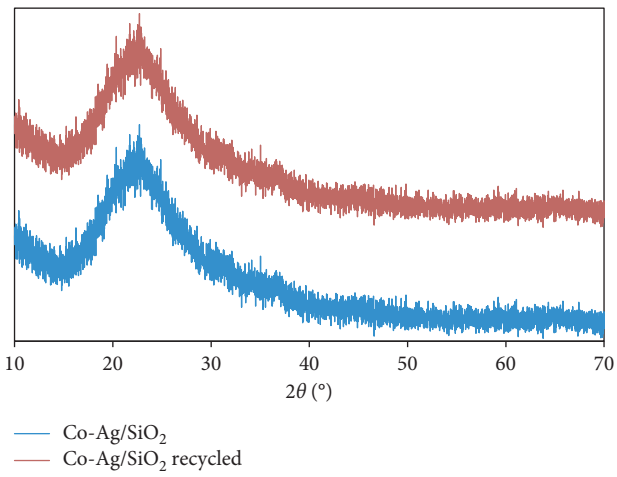

Figure 1: XRD patterns of fresh and recycled 1 mol% Co-1 mol% Ag supported SiO_2.

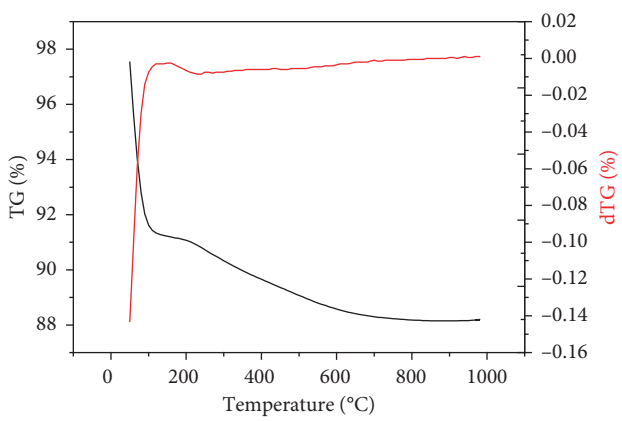

Figure 2: TG-DTG curve of 1 mol% Co-1 mol% Ag supported SiO_2.

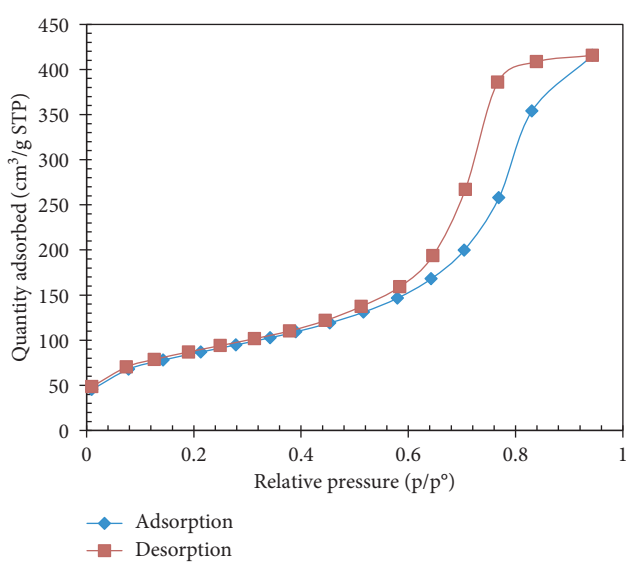

Figure 3: N adsorption/desorption isotherms of 1 mol% Co-1 mol % Ag supported SiO_2.

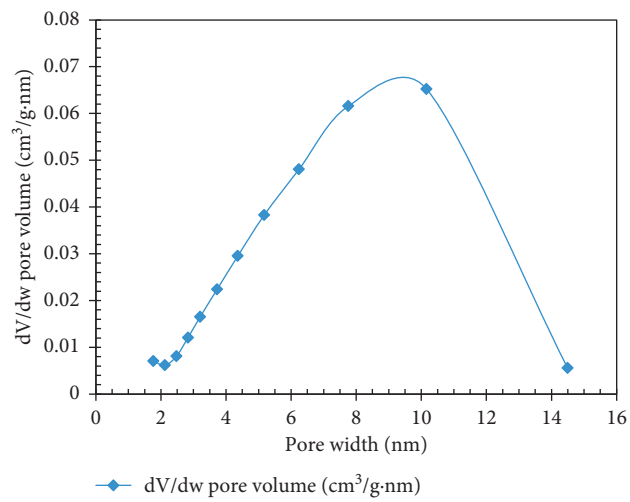

Figure 4: Distribution of the pore diameter of 1 mol% Co-1 mol% Ag supported SiO_2.

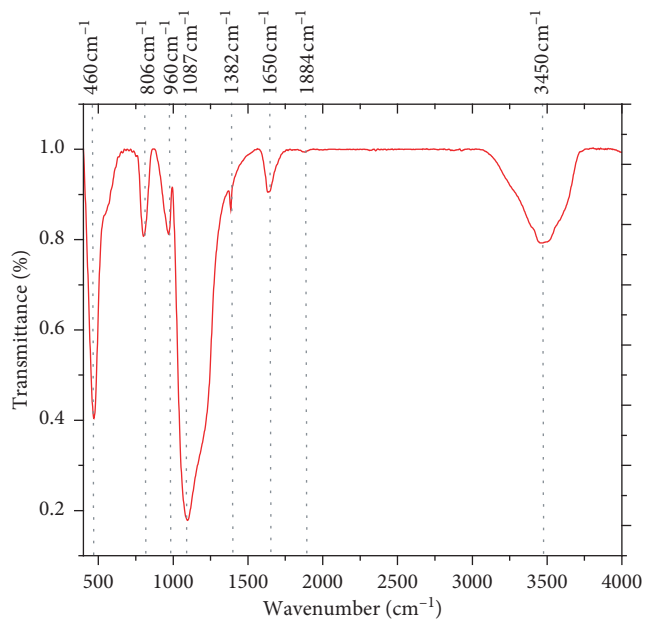

Figure 5: FT-IR spectrum of 1 mol% Co-1 mol% Ag supported SiO_2.

broad and intense at 3450 cm^{-1} are attributed to the presence of OH groups in the silica framework [40].

The scanning electron microscopy (SEM) of 1 mol% Co-1 mol% Ag supported on the SiO_2 catalyst and pure SiO_2 are shown in Figure 6. The amount of silver and cobalt codoped in SiO_2 do not change the morphology compared to its support. EDX results confirm that codoped and undoped SiO_2 nanopowders consist of elements of silicon, cobalt, and silver (Figure 6) in good agreement with the literature [41, 42] and providing further evidence for the successful synthesis of our nanocatalyst.

Element distribution in the hybrid has been carried out for 1 mol% Co-1 mol% Ag supported SiO_2 (Figure 7). All the elements representing our prepared catalyst were studied and showed a good distribution. For cobalt and silver, the

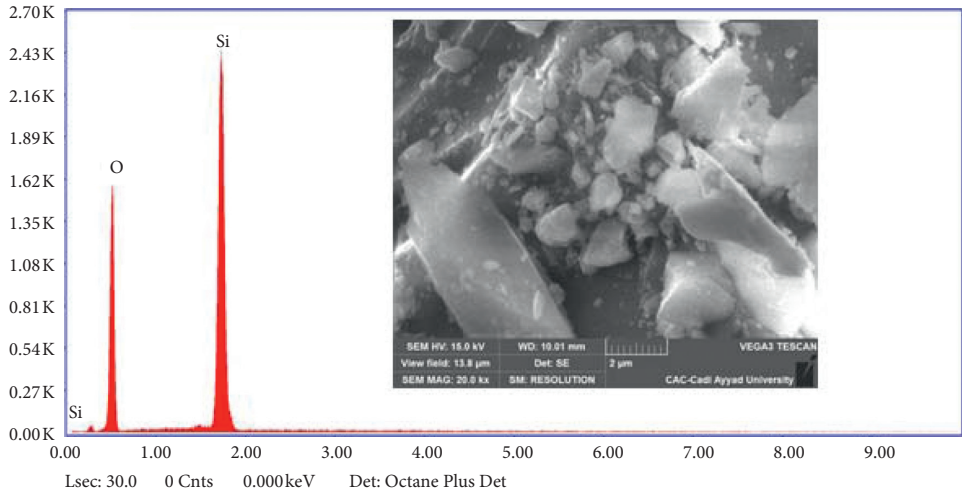

(a)

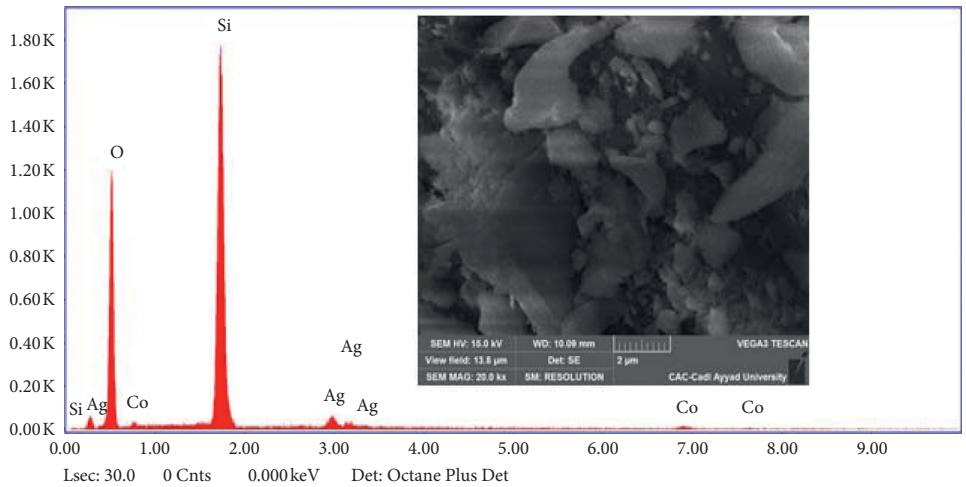

(b)

Figure 6: SEM images of (a) pure SiO_2 and (b) 1 mol% Co-1 mol% Ag supported SiO2.

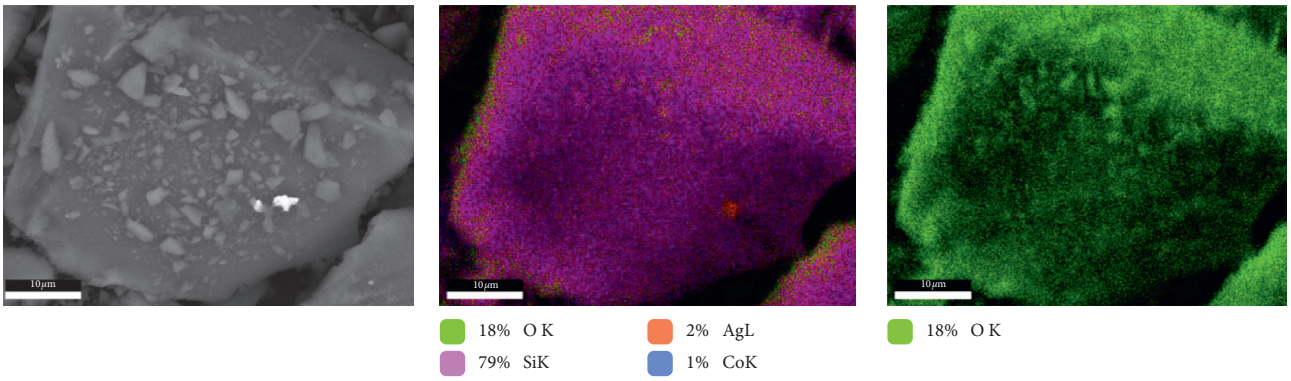

(a) (b) (c)

Figure 7: Continued.

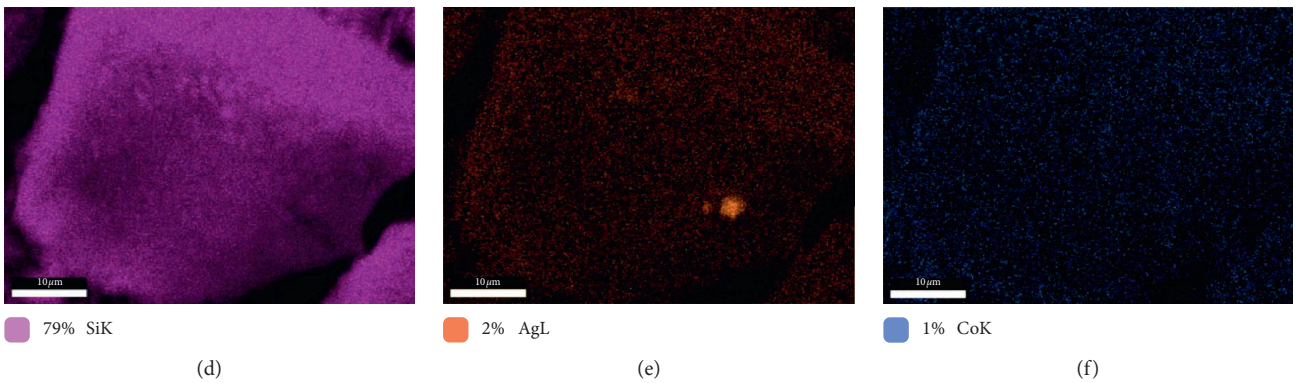

Figure 7: EDX elemental mapping analysis of 1 mol% Co-1 mol% Ag supported SiO_2: (a) the studied area and the distribution of (b) all elements, (c) oxygen, (d) silicon, (e) silver, and (f) cobalt.

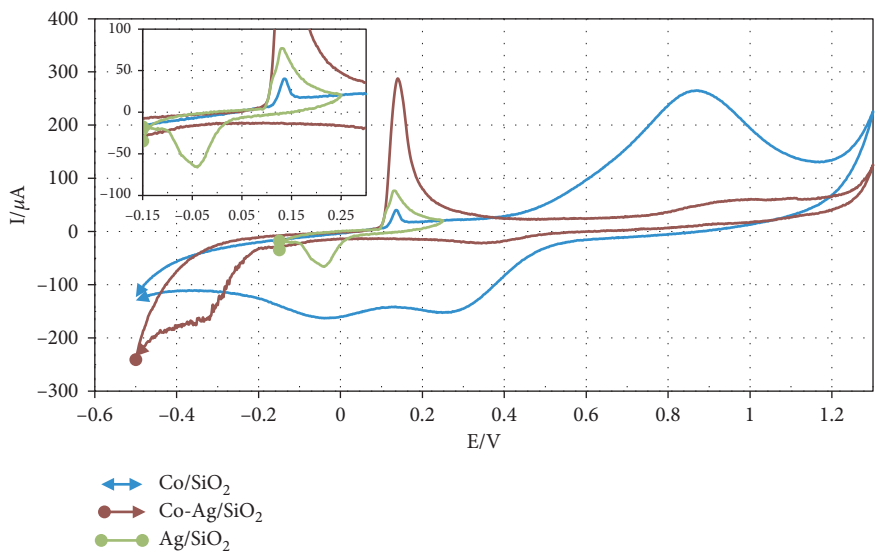

Figure 8: CV curves of carbon paste electrode modified with Co/SiO_2, $Co\text{-}Ag/SiO_2$ (performed between 1500 mV and 500 mV) and Ag/SiO_2 (performed between 300 mV/−200 mV) at a scan rate of 100 mV·s^{-1}.

studied area shows a good dispersion and distribution in a nanoscale range.

In order to study the metal predominant oxidation state of supported catalyst, cyclic voltammetry (CV) experiments represent a good alternative [29]. CV was performed for both the 1 mol% Co-1 mol% Ag supported SiO_2 prepared nanocatalyst and the monometallic supported silica Co/SiO_2 and Ag/SiO_2 (Figure 8). The study of cobalt and silver electrodes presents two specific zones of surface oxide formation and reduction. The monometallic Ag/SiO_2 redox voltammetric profile presents an anodic peak at 0.13 V (Ag^0-->Ag^+) and a cathodic peak at −0.04 V (Ag^+-->Ag^0), while the monometallic Co/SiO_2 shows the characteristic redox peaks of Co_3O_4 [43]. Moreover, the prepared 1 mol% Co-1 mol% Ag supported SiO_2 ($Co\text{-}Ag/SiO_2$) shows, in addition to the characteristic redox voltammetric profile of Co_3O_4, an anodic peak at 0.13 V with no obvious cathodic peak which confirms the presence of metallic silver (Ag^0). Therefore, the CV study indicates the presence of cobalt and silver under the Co_3O_4 and Ag^0 oxidation state, respectively.

3.2. Catalytic Application. The catalytic performance of the Co-Ag supported SiO_2 was examined by assessing the oxidation of α-pinene **1** chosen as a model substrate (Scheme 1). The reaction was optimized by varying the catalyst amount, reaction time, effect of temperature, and the nature of solvent.

3.2.1. Effect of Catalyst Amount. The catalytic oxidation of α-pinene **1** using hydrogen peroxide was performed by varying the amount (0.02 g to 0.15 g) of 1 mol% Co-1 mol% Ag supported SiO_2 (Table 1). The conversion of α-pinene **1** resulted in the increase of the catalyst amount. The best result was obtained with the 0.1 g nanocatalyst, and a conversion of 82% and a yield of 55% for both verbenol and verbenone are

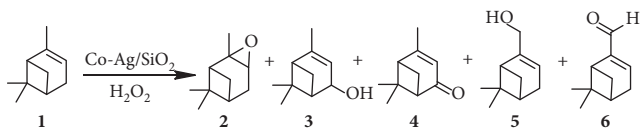

Scheme 1: Catalytic oxidation of α-pinene **1** using Co-Ag supported SiO_2.

Table 1: Effect of catalyst amount.

Amount of catalyst (g)	Conversion (%)	Yield (%)				
		Epoxide **2**	Verbenol **3**	Verbenone **4**	Myrtenol **5**	Myrtenal **6**
0.02	16	Trace	Trace	5.7	9	Trace
0.05	78.5	Trace	36.6	27.4	Trace	Trace
0.1	82	Trace	27	28	10	Trace
0.15	98	Trace	13	41	17	11

Reaction conditions: 0.5 mL α-pinene and 1.3 mL H_2O_2; 60°C; acetonitrile (5 ml); 24 h. Yields are determined by GC using dodecane as internal standard.

Table 2: Effect of reaction time.

Time (h)	Conversion (%)	Yield (%)				
		Epoxide **2**	Verbenol **3**	Verbenone **4**	Myrtenol **5**	Myrtenal **6**
6	42	7	11	24	0	0
12	48	12	11	25	0	0
20	78	14	11	42	4	2
24	100	2	12	50	7	20

Reaction conditions: 0.5 mL α-pinene **1**, 1.3 mL H_2O_2; 0.1 g catalyst; 80°C; acetonitrile (5 ml); 24 h. Yields are determined by GC using dodecane as internal standard.

reached. In the absence of the catalyst, no reaction took place even after stirring for a long reaction time.

3.2.2. Effect of the Reaction Time. In order to shed more light on this point, a kinetic study was carried out with 1 mol% Co-1 mol% Ag supported SiO_2 (Table 2). Based on these results, the evolution of α-pinene **1** versus time shows that verbenone was formed as a major product. A total conversion of α-pinene **1** was reached after 24 hours with 50% of verbenone and 20% of myrtenal yields, respectively.

3.2.3. Effect of Reaction Temperature. Table 3 shows the influence of the temperature on the catalytic oxidation of α-pinene **1**. The increase of the temperature to 120°C resulted in the increase of the conversion and the selectivity to verbenone decreases due to the formation of isomerization products and the opening of the cyclobutane ring. This confirms that the cleavage of the C=C bond is greater at lower temperatures and the opening of the cyclobutane ring and isomerization reactions is more favorable than the C=C cleavage at high temperatures [16].

3.2.4. Effect of the Solvent. In order to evaluate the catalytic performance of Co-Ag supported SiO_2, an examination of the effect of various protic and aprotic solvents in the presence of hydrogen peroxide (30 wt%) has been carried out (Table 4).

According to Table 4, polar and aprotic solvents (acetonitrile and acetone) are more active and selective towards verbenone. In the presence of polar and protic solvents (methanol and ethanol), the selectivity increases towards verbenol while in the absence of solvent, the α-pinene **1** is completely converted, and a low yield of verbenone (30%) was obtained with the formation of isomerization products and the opening cyclobutane ring. Among the solvents used, acetonitrile seems to be the best solvent.

3.2.5. Co-Ag/SiO_2 Catalytic Performance. Under the optimized conditions, catalytic oxidation of various terpenic olefins has been carried out (Table 5). As shown in Table 5, limonene was converted to the corresponding allylic ketone, carvone as the major compound (entry 1). However, β-pinene leads to the formation of myrtenal as a major product (entry 2). Performing the reaction with valencene resulted in a total conversion and gave, mainly, nootkatone in the 80% yield (entry 3).

3.2.6. Effect of TBHP. The catalytic oxidation of various terpenic olefins using *tert*-butyl hydroperoxide (TBHP 70%), a nonpolluting and economic oxidant agent [5, 18], has been carried out (Table 6). All the terpenic olefins show good activities, and the corresponding ketones were obtained in a moderate-to-good yield. As shown in Table 6, it appeared that limonene and β-pinene (entries 5 and 6) were less reactive compared to α-pinene and valencene (entries 4 and 7).

Table 3: Effect of reaction temperature.

Temperature (°C)	Conversion (%)	Yield (%)				
		Epoxide **2**	Verbenol **3**	Verbenone **4**	Myrtenol **5**	Myrtenal **6**
R.T	0	0	0	0	0	0
60	80	4	20	29	3	4
80	100	2	12	50	7	20
100	95	4	7	33	6	8
120	96	4	12	44	2	5

Reaction conditions: 0.5 mL α-pinene, 1.3 mL H_2O_2; catalyst 0.1 g; 24 h; acetonitrile (5 ml). Yields are determined by GC using dodecane as internal standard.

Table 4: Effect of solvent.

Solvent	Conversion (%)	Yield (%)				
		Epoxide **2**	Verbenol **3**	Verbenone **4**	Myrtenol **5**	Myrtenal **6**
Free solvent	100	7	16	30	6	Trace
Ethanol	100	5	31	37	6	2
Methanol	94	15	59	13	Trace	2
Chloroforme	40	11	25	5	Trace	Trace
Acetone	98	7	6	46	3	14
Acetonitrile	100	2	12	50	7	20

Reaction conditions: 0.5 mL α-pinene, 1.3 mL H_2O_2; catalyst 0.1 g; 80°C; 24 h. Yields are determined by GC using dodecane as internal standard.

Table 5: Catalytic oxidation of terpenic olefins.

Entry	Substrate	Conv. (%)	Yield (%)				
1	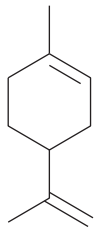	56	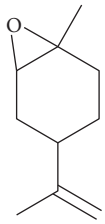 10%	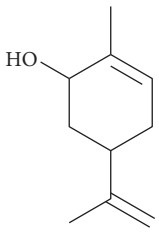 12%	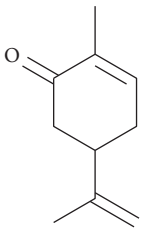 34%		
2	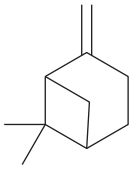	95	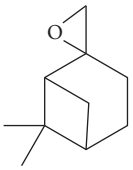 Trace	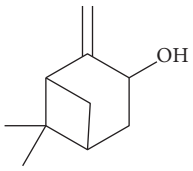 21%	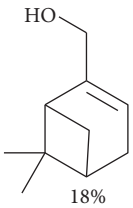 18%	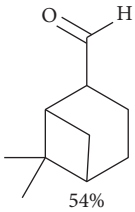 54%	
3	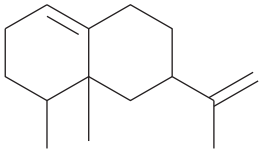	100	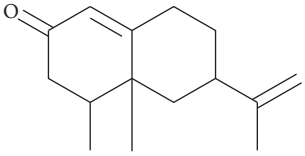 80%				

Reaction conditions: 0.5 mL substrate, 1.5 mL H_2O_2; catalyst 0.1 g; 80°C; acetonitrile; 24 h. Yields are determined by GC using dodecane as internal standard.

3.2.7. Recycling of Catalyst. To investigate the reusability of the 1 mol% Co-1 mol% Ag supported SiO_2 nanocatalyst, the catalytic performance was evaluated in four consecutive cycles (Figure 9). After each cycle, the catalyst was separated from the reaction mixture by simple filtration, washed with water, and dried at 200°C for 2 hours while being reused. According to Figure 9, the catalyst was stable after four cycles. Investigation of XRD analysis shows that the identity of the recovered Co-Ag/SiO_2 remains similar to the fresh nanocatalyst (Figure 1). However, SEM morphology of the nanocatalyst after four cycles showed some agglomerated particles compared to the fresh one (Figure 10). Moreover,

Table 6: Effect of TBHP.

Entry	Substrate	Conv. (%)	Yield (%)				
4	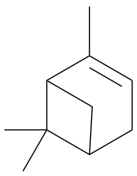	98	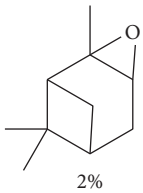 2%	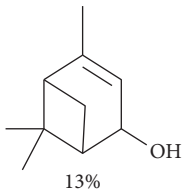 13%	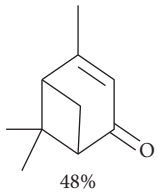 48%	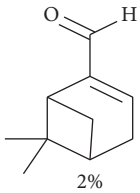 2%	
5	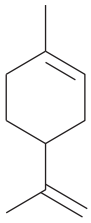	72	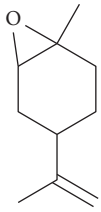 4%	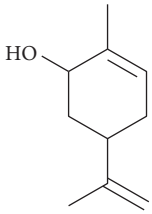 6%	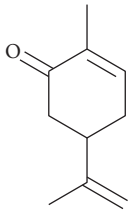 18%		
6	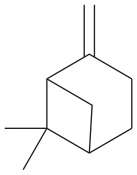	72	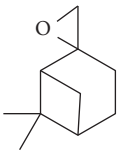 10%	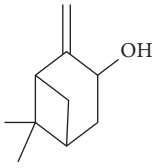 4%	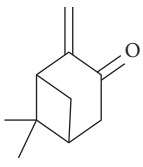 12%	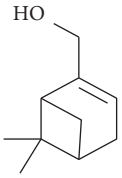 18%	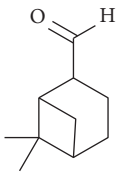 10%
7	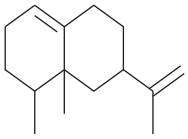	100	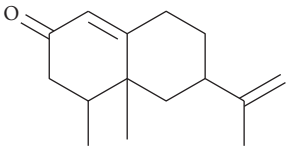 87%				

Reaction conditions: 0.5 mL substrate, 1.5 mL TBHP; catalyst 0.1 g; 80°C; acetonitrile (5 ml); 24 h. Yields are determined by GC using dodecane as internal standard.

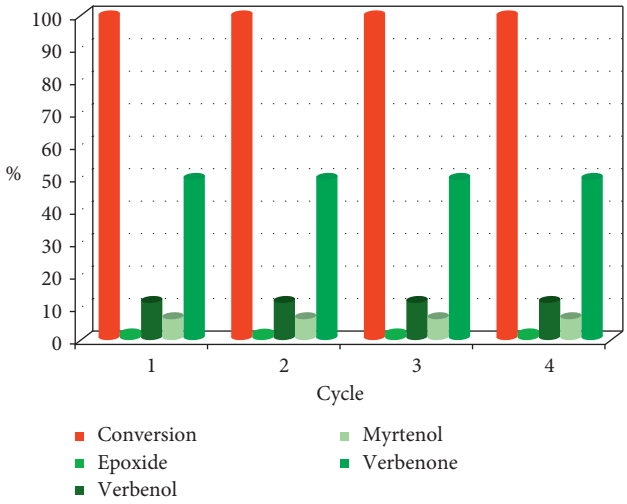

Figure 9: Oxidation of α-pinene during recyclability of 1 mol% Co-1 mol% Ag supported SiO_2.

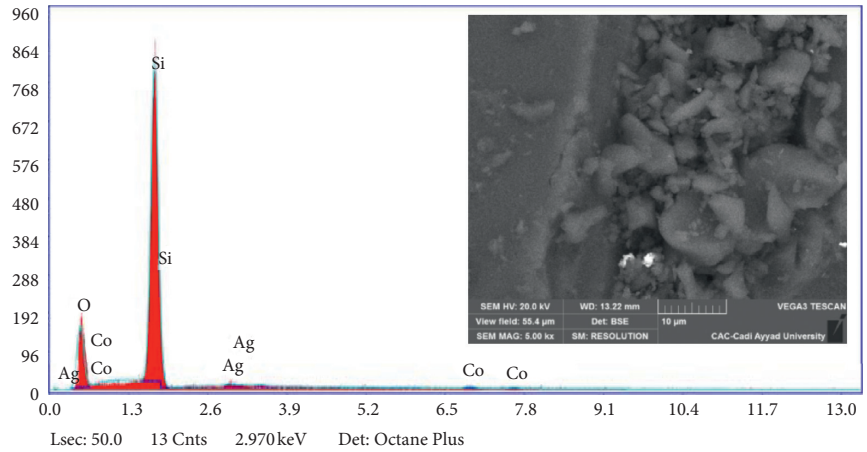

(a)

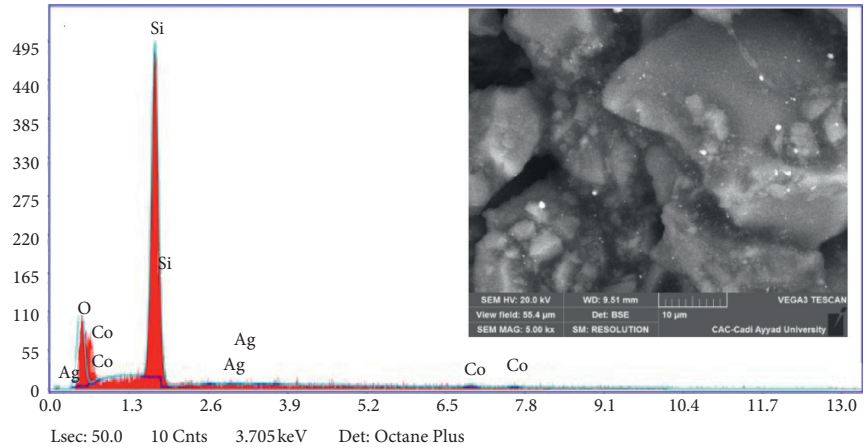

(b)

Figure 10: SEM images of (a) fresh and (b) recycled 1 mol% Co-1 mol% Ag supported SiO_2.

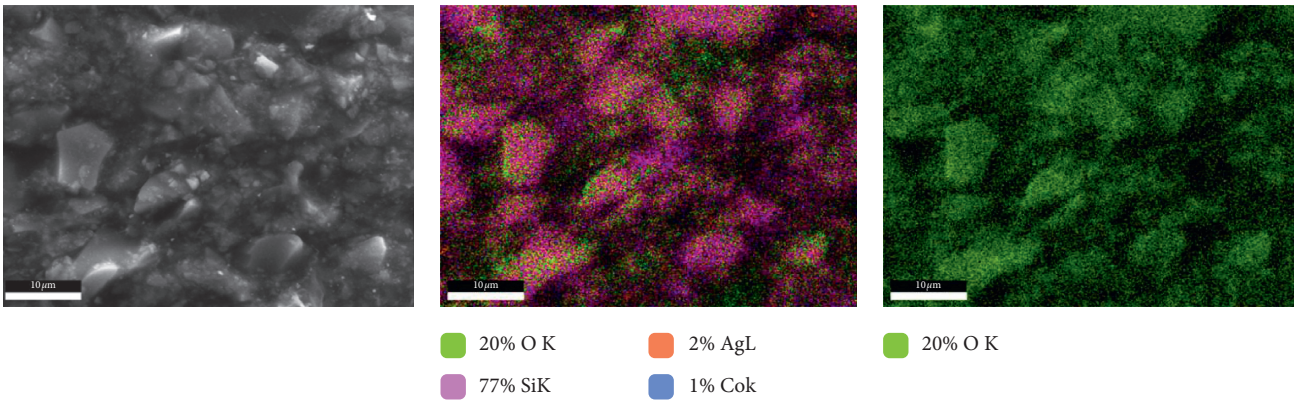

(a) (b) (c)

Figure 11: Continued.

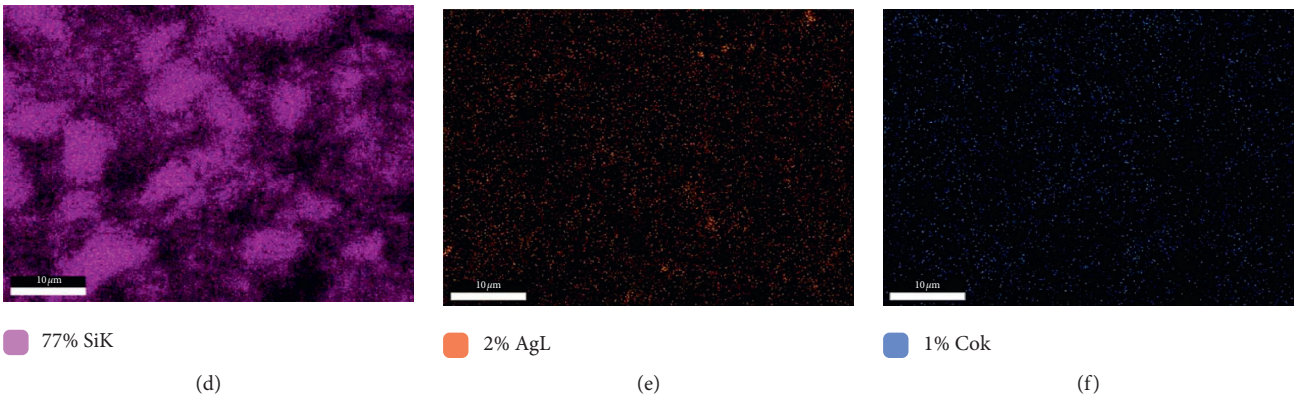

Figure 11: EDX elemental mapping analysis of recycled 1 mol% Co-1 mol% Ag supported SiO_2 after four cycles: (a) the studied area and the distribution of (b) all elements, (c) oxygen, (d) silicon, (e) silver, and (f) cobalt.

EDX elemental mapping of recycled Co-Ag/SiO_2 indicates no changes of dispersion and distribution of all elements compared to the fresh nanocatalyst (Figure 11).

4. Conclusion

The 1 mol% Co-1 mol% Ag supported SiO_2 catalyst prepared by the sol-gel method is an efficient and recyclable catalyst. The prepared catalyst shows a significant activity, a good reusability, and stability towards the oxidation of terpenic olefins using hydrogen peroxide and *tert*-butyl peroxide as green oxidizing agents. In the presence of H_2O_2, the prepared catalyst showed a high selectivity towards ketones and aldehydes in good yields. However, in the presence of TBHP, the reaction leads to the formation of ketones and aldehydes with a loss of selectivity and yields. The investigation of the recycled catalyst indicates that the recovered Co-Ag/SiO_2 remains similar to the fresh one in terms of catalytic yields, morphology, dispersion, and distribution over four consecutive cycles.

Data Availability

SEM/EDX, FT-IR, XRD, TG-DTG, BET, CV, and the device types used for recording spectra and other analytical data used to support the findings of this study are included in the manuscript.

Disclosure

This work was part of a thesis work of a PhD student.

Conflicts of Interest

The authors declare that they have no conflicts of interest.

References

[1] NR. Council, *Catalysis Looks to the Future*, National Academies Press, Washington, DC, USA, 1st edition, 1992.

[2] S. Senkan, "Combinatorial heterogeneous catalysis-a new path in an old field," *Angewandte Chemie International Edition*, vol. 40, no. 2, pp. 312–329, 2001.

[3] I. W. C. E. Arends, R. A. Sheldon, M. Wallau, and U. Schuchardt, "Oxidative transformations of organic compounds mediated by redox molecular sieves," *Angewandte Chemie International Edition in English*, vol. 36, no. 11, pp. 1144–1163, 1997.

[4] A. S. Kumar, B. Thulasiram, S. B. Laxmi, V. S. Rawat, and B. Sreedhar, "Magnetic $CuFe_2O_4$ nanoparticles: a retrievable catalyst for oxidative amidation of aldehydes with amine hydrochloride salts," *Tetrahedron*, vol. 70, no. 36, pp. 6059–6067, 2014.

[5] H. E. B. Lempers and R. A. Sheldon, "Allylic oxidation of olefins to the corresponding α,β-unsaturated ketones catalyzed by chromium aluminophosphate-5," *Applied Catalysis A: General*, vol. 143, no. 1, pp. 137–143, 1996.

[6] D. Avnir, "Organic chemistry within ceramic matrixes: doped sol-gel materials," *Accounts of Chemical Research*, vol. 28, no. 8, pp. 328–334, 1995.

[7] C.-C. Wang and J. Y. Ying, "Sol-gel synthesis and hydrothermal processing of anatase and rutile titania nanocrystals," *Chemistry of Materials*, vol. 11, no. 11, pp. 3113–3120, 1999.

[8] P. A. Robles-Dutenhefner, M. J. da Silva, L. S. Sales, E. M. B. Sousa, and E. V. Gusevskaya, ""Solvent-free liquid-phase autoxidation of monoterpenes catalyzed by sol–gel Co/SiO_2," *Journal of Molecular Catalysis A: Chemical*, vol. 217, no. 1-2, pp. 139–144, 2004.

[9] F. Temelli, R. J. Braddock, C. S. Chen, and S. Nagy, "Supercritical carbon dioxide extraction of terpenes from orange essential oil," *ACS Symposium Series*, vol. 366, pp. 109–126, 1988.

[10] M. Rauchdi, M. Ait Ali, A. Roucoux, and A. Denicourt-Nowicki, "Novel access to verbenone via ruthenium nanoparticles-catalyzed oxidation of α-pinene in neat water," *Applied Catalysis A: General*, vol. 550, pp. 266–273, 2018.

[11] J. A. Gonçalves and E. V. Gusevskaya, "Palladium catalyzed oxidation of monoterpenes: multistep electron transfer catalytic systems $Pd(OAc)_2$/benzoquinone/$M(OAc)_2$ (M=Cu, Co or Mn) for the allylic oxidation of limonene with dioxygen," *Applied Catalysis A: General*, vol. 258, no. 1, pp. 93–98, 2004.

[12] D. H. Pybus and C. S. Sell, *Chemistry, the Chemistry of Fragrances*, Royal Society of Chemistry, London, UK, 1st edition, 1999.

[13] P. A. Wender and T. P. Mucciaro, "A new and practical approach to the synthesis of taxol and taxol analogs: the pinene path," *Journal of the American Chemical Society*, vol. 114, no. 14, pp. 5878-5879, 1992.

[14] P. E. Shaw and C. W. Wilson III, "Importance of nootkatone to the aroma of grapefruit oil and the flavor of grapefruit juice," *Journal of Agricultural and Food Chemistry*, vol. 29, no. 3, pp. 677–679, 1981.

[15] T. Yanami, M. Miyashita, and A. Yoshikoshi, "Synthetic study of (+)-nootkatone from (-)-.beta.-pinene," *The Journal of Organic Chemistry*, vol. 45, no. 4, pp. 607–612, 1980.

[16] B. A. Allal, L. El Firdoussi, S. Allaoud, A. Karim, Y. Castanet, and A. Mortreux, "Catalytic oxidation of α-pinene by transition metal using t-butyl hydroperoxide and hydrogen peroxide," *Journal of Molecular Catalysis A: Chemical*, vol. 200, no. 1-2, pp. 177–184, 2003.

[17] L. El Firdoussi, A. Baqqa, S. Allaoud et al., "Selective palladium-catalysed functionalization of limonene: synthetic and mechanistic aspects," *Journal of Molecular Catalysis A: Chemical*, vol. 135, no. 1, pp. 11–22, 1998.

[18] E. F. Murphy, T. Mallat, and A. Baiker, "Allylic oxo-functionalization of cyclic olefins with homogeneous and heterogeneous catalysts," *Catalysis Today*, vol. 57, no. 1-2, pp. 115–126, 2000.

[19] M. Islam, D. Hossain, P. Mondal, A. S. Roy, S. Mondal, and M. Mobarak, "Selective oxidation of olefins catalyzed by polymer-anchored nickel(II) complex in water medium," *Bulletin of the Korean Chemical Society*, vol. 31, no. 12, pp. 3765–3770, 2010.

[20] M. Lajunen and A. M. P. Koskinen, "Co (II)-catalysed allylic oxidation of α-pinene by molecular oxygen; synthesis of verbenone," *Tetrahedron Letters*, vol. 35, no. 25, pp. 4461–4464, 1994.

[21] S. Ajaikumar, J. Ahlkvist, W. Larsson et al., "Oxidation of α-pinene over gold containing bimetallic nanoparticles supported on reducible TiO_2 by deposition-precipitation method," *Applied Catalysis A: General*, vol. 392, no. 1-2, pp. 11–18, 2011.

[22] P. A. Robles-Dutenhefner, B. B. N. S. Brandão, L. F. De Sousa, and E. V. Gusevskaya, "Solvent-free chromium catalyzed aerobic oxidation of biomass-based alkenes as a route to valuable fragrance compounds," *Applied Catalysis A: General*, vol. 399, no. 1-2, pp. 172–178, 2011.

[23] M. Selvaraj, M. Kandaswamy, D. W. Park, and C. S. Ha, "Highly efficient and clean synthesis of verbenone over well ordered two-dimensional mesoporous chromium silicate catalysts," *Catalysis Today*, vol. 158, no. 3-4, pp. 286–295, 2010.

[24] N. R. Kim, K. Shin, I. Jung, M. Shim, and H. M. Lee, "Ag-Cu bimetallic nanoparticles with enhanced resistance to oxidation: a combined experimental and theoretical study," *The Journal of Physical Chemistry C*, vol. 118, no. 45, pp. 26324–26331, 2014.

[25] J. Sopousek, J. Pinkas, P. Broz et al., "Ag-Cu colloid synthesis: bimetallic nanoparticle characterisation and thermal treatment," *Journal of Nanomaterials*, vol. 2014, Article ID 638964, 13 pages, 2014.

[26] G. Sharma, A. Kumar, M. Naushad, D. Pathania, and M. Sillanpää, "Polyacrylamide@Zr(IV) vanadophosphate nanocomposite: ion exchange properties, antibacterial activity, and photocatalytic behavior," *Journal of Industrial and Engineering Chemistry*, vol. 33, pp. 201–208, 2016.

[27] N. Toshima and T. Yonezawa, "Bimetallic nanoparticles-novel materials for chemical and physical applications," *New Journal of Chemistry*, vol. 22, no. 11, pp. 1179–1201, 1998.

[28] A. Aberkouks, A. A. Mekkaoui, B. Boualy, S. El Houssame, M. Ait Ali, and L. El Firdoussi, "Selective oxidation of styrene to benzaldehyde by Co-Ag codoped ZnO catalyst and H_2O_2 as oxidant," *Advances in Materials Science and Engineering*, vol. 2018, Article ID 2716435, 7 pages, 2018.

[29] A. A. Mekkaoui, S. Jennane, A. Aberkouks et al., "Palladium nanoparticles supported on mesoporous natural phosphate: an efficient recyclable catalyst for nitroarene reduction," *Applied Organometallic Chemistry*, vol. 33, no. 10, p. e5117, 2019.

[30] A. Aberkouks, A. A. Mekkaoui, B. Boualy, S. El Houssame, M. Ait Ali, and L. El Firdoussi, "Co-Ag supported ZnO: an efficient and recyclable heterogeneous catalyst for the oxidation of natural terpenes," *Materials Today: Proceedings*, vol. 13, no. 3, pp. 453–457, 2019.

[31] J. Bang, *Effects of Excitation Density and Energy Transfer on Cathodoluminescence from Powder Phosphors with and without Embedded Nanoparticles*, George A. Smathers Libraries, Gainesville, FL, USA, 1st edition, 2004.

[32] O. M. Ntwaeaborwa and P. H. Holloway, "Enhanced photoluminescence of Ce^{3+} induced by an energy transfer from ZnO nanoparticles encapsulated in SiO_2," *Nanotechnology*, vol. 16, no. 6, pp. 865–868, 2005.

[33] O. M. Ntwaeaborwa, H. C. Swart, R. E. Kroon, P. H. Holloway, and J. R. Botha, "Photoluminescence of cerium europium co-doped SiO_2 phosphor prepared by a sol–gel process," *Surface and Interface Analysis*, vol. 38, no. 4, pp. 458–461, 2006.

[34] L. G. Ceballos-Mendivil, R. E. Cabanillas-López, J. C. Tánori-Córdova et al., "Synthesis of silicon carbide using concentrated solar energy," *Solar Energy*, vol. 116, pp. 238–246, 2015.

[35] B. B. F. Mirjalili and L. Zamani, "Nano-$TiCl_4$. SiO_2: a versatile and efficient catalyst for synthesis of dihydropyrimidones via Biginelli condensation," *South African Journal of Chemistry*, vol. 67, pp. 21–26, 2014.

[36] A. N. Scian and C. Volzone, "Novel SiO_2-C composite adsorptive material," *Boletín de la Sociedad Española de Cerámica y Vidrio*, vol. 40, no. 4, pp. 279–284, 2001.

[37] H. Jung, R. Gupta, E. Oh, Y. Kim, and C. Whang, "Vibrational spectroscopic studies of sol–gel derived physical and chemical bonded ORMOSILs," *Journal of Non-crystalline Solids*, vol. 351, no. 5, pp. 372–379, 2005.

[38] J. Roman, S. Padilla, and M. Vallet-Regi, ""Sol–gel glasses as precursors of bioactive glass ceramics," *Chemistry of Materials*, vol. 15, no. 3, pp. 798–806, 2003.

[39] B. C. Smith, *Infrared Spectral Interpretation: A Systematic Approach*, CRC Press, Boca Raton, FL, USA, 1st Edition, 1998.

[40] R. M. Almeida and C. G. Pantano, "Structural investigation of silica gel films by infrared spectroscopy," *Journal of Applied Physics*, vol. 68, no. 8, pp. 4225–4232, 1990.

[41] J. F. P. Liévano and L. A. C. Díaz, "Synthesis and characterization of 1-methyl-3-methoxysilyl propyl imidazolium chloride mesoporous silica composite as adsorbent for dehydration in industrial processes," *Materials Research*, vol. 19, no. 3, pp. 534–541, 2016.

[42] L. Morejón-Alonso, R. G. Carrodeguas, and L. A. dos Santos, "Effects of silica addition on the chemical, mechanical and biological properties of a new tricalcium phosphate/tricalcium silicate cement," *Materials Research*, vol. 14, no. 4, pp. 475–482, 2011.

[43] A. Aljabour, H. Coskun, D. H. Apaydin et al., "Nanofibrous cobalt oxide for electrocatalysis of CO_2 reduction to carbon monoxide and formate in an acetonitrile-water electrolyte solution," *Applied Catalysis B: Environmental*, vol. 229, pp. 163–170, 2018.